International Journal of Mechanical, Industrial and Aerospace Sciences
ISSN: 2517-9950
Vol:5, No:9, 2011

Anisotropic Constitutive Model and its Application in Simulation of Thermal Shock Wave Propagation for Cylinder Shell Composite

Xia Huang, Wenhui Tang, Banghai Jiang, and Xianwen Ran

***Abstract*—**In this paper, a plane-strain orthotropic elasto-plastic dynamic constitutive model is established, and with this constitutive model, the thermal shock wave induced by intense pulsed X-ray radiation in cylinder shell composite is simulated by the finite element code, then the properties of thermal shock wave propagation are discussed. The results show that the thermal shock wave exhibit different shapes under the radiation of soft and hard X-ray, and while the composite is radiated along different principal axes, great differences exist in some aspects, such as attenuation of the peak stress value, spallation and so on.

***Keywords*—**anisotropic constitutive model, thermal shock wave, X-ray, cylinder shell composite.

I. Introduction

WHILE a material is radiated by intense pulsed X-ray, a great deal of energy rapidly deposits in the material surface, and huge temperature and pressure gradients are formed due to the fast attenuation of deposited energy from surface to inner. Simultaneously, the adiabatic expansion occurs with the quick increase of specific internal energy, and if the incident energy fluence is high enough to exceed the sublimation energy of material,, the radiated material surface will sublimate to gas immediately, then the blow-off effect on the material takes place due to the forth ejection of gas. Thus a thermal shock wave is formed by these factors [1]. When the thermal shock wave propagates to the interface with low resistance or the free surface, a reflected release wave will be generated for the release of thermal shock wave. With the interaction between the reflected release wave and the rarefaction part of incident thermal shock wave, an intense tensile effect occurs which results in the material spallation destruction [2]. Because of the difficulty of intense pulsed X-ray radiation experiment, numerical simulation is a main method to study the thermal shock wave induced by X-ray radiation. For many years, many relevant jobs were confined to numerical simulation of metal materials by using the ideal elasto-plastic constitutive model. With the wide application of composite materials, it is of great significance to study the rules of thermal shock wave propagation induced by pulsed X-ray. When the side surface of cylinder shell structure is radiated by X-ray, the thermodynamic response can be simplified as a plane-strain model [3]. But most composite materials are anisotropic, and the thermodynamic response is rate-related. So, when we research on the shock wave propagation in composite, establishing the anisotropic dynamic elasto-plastic constitutive model is very important to enhance the validity of numerical simulation.

In this paper, taking the carbon fiber-reinforced phenolic composite (hereinafter simply referred as TF) for example, a plane-strain orthotropic dynamic constitutive model which considers elasto-plastic deformation, strain rate sensitivity, strain hardening effect, and nonlinear property of volume change in both compression and expansion states is established. With this constitutive model, a finite element program is made to simulate the thermal shock wave propagation in cylinder shell composite under soft and hard X-ray radiation, and the thermal shock wave propagation properties are discussed.

II. Plane-strain Constitutive Model for Elastic Response

For orthotropic composite material, there are three principal axis directions (use 1, 2, 3 denotation), and invoking the condition of plane strain (1-2 plane for example), we get $\varepsilon_{33} = \varepsilon_{13} = \varepsilon_{23} = 0$ and $\sigma_{13} = \sigma_{23} = 0$.

In the elastic deformation phase, the stress-strain relation is described by Hooke law:

$$\begin{cases} \sigma_{11} = c_{11}\varepsilon_{11} + c_{12}\varepsilon_{22} \\ \sigma_{22} = c_{12}\varepsilon_{11} + c_{22}\varepsilon_{22} \\ \sigma_{33} = c_{13}\varepsilon_{11} + c_{23}\varepsilon_{22} \\ \sigma_{12} = c_{44}\varepsilon_{12} \end{cases} \quad (1)$$

Where

X. Huang is with Institute of Technological Physics, College of Science, National University of Defense Technology, Changsha 410073 China (e-mail: hx_1984.4@163.com).

W. Tang is with Institute of Technological Physics, College of Science, National University of Defense Technology, Changsha 410073 China (corresponding author to provide phone: 86-0731-84573268; fax: 86-0731-84573268; e-mail: wenhuitang@163.com).

B. Jiang is with Institute of Technological Physics, College of Science, National University of Defense Technology, Changsha 410073 China (e-mail: jbhnudt@yahoo.com).

X. Ran is with Institute of Technological Physics, College of Science, National University of Defense Technology, Changsha 410073 China (e-mail: ranxianwen@163.com).

This work was supported by the National Natural Science Foundation of China under Grant No. 11072262.

$$c_{11}=E_1\left(1-\upsilon_{23}^2\frac{E_3}{E_2}\right)/\alpha\ ,\ c_{22}=E_2\left(1-\upsilon_{13}^2\frac{E_3}{E_1}\right)/\alpha\ ,$$
$$c_{33}=E_3\left(1-\upsilon_{12}^2\frac{E_2}{E_1}\right)/\alpha\ ,\ c_{12}=E_2\left(\upsilon_{12}+\upsilon_{13}\upsilon_{23}\frac{E_3}{E_2}\right)/\alpha\ ,$$
$$c_{13}=E_3\left(\upsilon_{13}+\upsilon_{12}\upsilon_{23}\right)/\alpha\ ,\ c_{23}=E_3\left(\upsilon_{23}+\upsilon_{12}\upsilon_{13}\frac{E_2}{E_1}\right)/\alpha\ ,$$
$$c_{44}=2G_{12}\ ,\ \alpha=1-\upsilon_{12}^2\frac{E_2}{E_1}-\upsilon_{13}^2\frac{E_3}{E_1}-\upsilon_{23}^2\frac{E_3}{E_2}-2\upsilon_{12}\upsilon_{13}\upsilon_{23}\frac{E_3}{E_1}\ ,$$

E_i's are the Young's moduli, G_{ij}'s are the shear moduli, and υ_{ij}'s are the Poisson ratios.

To separate thermodynamic (equation of state) response from the ability of material to carry shear loads (strength), it is convenient to partition the strains into volumetric and deviatoric components. For plane-strain problem, under the condition of small strain, the volumetric strain $\theta\approx\varepsilon_{11}+\varepsilon_{22}$, and the deviatoric strains are expressed as the difference between total strain and volumetric strain:

$$\varepsilon_{ij}^d=\varepsilon_{ij}-\theta\delta_{ij}/3 \tag{2}$$

where ε_{ij}^d is the deviatoric strain component and δ_{ij} is the Kronecker delta function.

The total stress tensor is also decomposed into pressure and deviatoric stress component:

$$\sigma_{ij}=-p\delta_{ij}+s_{ij} \tag{3}$$

where pressure p is defined as the negative of mean stress which is the average of the three normal stress components, and s_{ij} is the deviatoric stress component.

Therefore, the pressure is:

$$\begin{aligned}p&=-\left(\sigma_{11}+\sigma_{22}+\sigma_{33}\right)/3\\&=-\left(c_{11}+3c_{12}+c_{13}+2c_{22}+2c_{23}\right)\theta/9\\&\quad-\left(c_{11}+c_{13}-c_{22}-c_{23}\right)\varepsilon_{11}^d/3\end{aligned} \tag{4}$$

It is clear that, for the anisotropic material, in addition to the volumetric strain, the pressure also depends on the deviatoric strain component. That is to say the pressure can result in shape deformation, and in the limit of isotropic material, (4) reduces to $p=-\kappa\theta=-E\theta/\left[3\left(1-2\upsilon\right)\right]$, where k is the bulk modulus, E is the Young's modulus, and υ is the Poisson ratio of isotropic material.The deviatoric stress components can be written as:

$$\begin{cases}s_{11}=\left(2c_{11}+3c_{12}-c_{13}-2c_{22}-2c_{23}\right)\theta/9\\\qquad+\left(2c_{11}-3c_{12}-c_{13}+c_{22}+c_{23}\right)\varepsilon_{11}^d/3\\s_{22}=\left(-c_{11}-c_{13}+4c_{22}-2c_{23}\right)\theta/9\\\qquad+\left(-c_{11}+3c_{12}-c_{13}-2c_{22}+c_{23}\right)\varepsilon_{11}^d/3\\s_{33}=\left(-c_{11}-3c_{12}+2c_{13}-2c_{22}+4c_{23}\right)\theta/9\\\qquad+\left(-c_{11}+2c_{13}+c_{22}-2c_{23}\right)\varepsilon_{11}^d/3\\s_{12}=c_{44}\varepsilon_{12}^d=c_{44}\varepsilon_{12}\end{cases} \tag{5}$$

But the linear relation in (4) is satisfied only at very low pressure. To calculate the nonlinear behaviour of volume change, the equation of state is introduced. Under background of intense X-ray radiation, the material state is very complex, and PUFF equation of state is often used to depict both the compressive shock state with relatively low temperature and the coupling state of energy deposition and fluid dynamics movement [3], which is written as:

compression region:

$$p=p_H(v)+\rho_0\Gamma_0\left(e-e_H\right) \tag{6}$$

expansion region:

$$\begin{aligned}p=\rho&\left[\gamma-1+\left(\Gamma_0-\gamma+1\right)\sqrt{\rho/\rho_0}\right]\\&\left[e-e_s\left\{1-\exp\left[N\rho_0\left(1-\rho_0/\rho\right)/\rho\right]\right\}\right]\end{aligned} \tag{7}$$

where p_H is Hugoniot pressure, v is specific volume, e is specific internal energy, Γ_0 is Grüneisen parameter, γ is adiabatic exponent, $N=c_0^2/(\Gamma_0 e_s)$, and e_s is sublimation energy. Equation (6) and (7) are continuous at $\rho=\rho_0$, and (7) can transit from solid state to gas state very well.

Equation (8) and (9) are the traditional PUFF equation of state, and they can be rewritten as a Taylor's series expansion of μ, where $\mu=\rho/\rho_0-1\approx\ -\theta$, so the following equations are gotten:

compression region:

$$\begin{aligned}p=&-A_1\theta+\left(A_2-A_1\Gamma_0/2\right)\theta^2\\&-\left(A_3-A_2\Gamma_0/2\right)\theta^3+\left(\rho_0\Gamma_0-\rho_0\Gamma_{0}\theta\right)e\end{aligned} \tag{8}$$

dilation region:

$$\begin{aligned}p=&-B_1\theta+B_2\theta^2-B_3\theta^3\\&+\left[\rho_0\Gamma_0-3\rho_0\Gamma_0\theta/2+\rho_0\left(\gamma-1\right)\theta/2\right]e\end{aligned} \tag{9}$$

where $A_1=\rho_0c_0^2$, $A_2=A_1\left(2s-1\right)$, $A_3=A_1\left(3s^2-4s+1\right)$, $B_1=\rho_0c_0^2$, $B_2=-B_1/2-B_1\left(\gamma-1\right)/2\Gamma_0+B_1N/2$, $B_3=\frac{5B_1}{24}+\frac{5}{8}\frac{\gamma-1}{\Gamma_0}B_1-\left(\frac{5}{4}+\frac{\gamma-1}{4\Gamma_0}\right)B_1N+\frac{1}{6}B_1N^2$. c_0 and s are the parameters gained from dynamic experiment.Equation (8) and (9) are the series forms of PUFF equation of state which are only suitable for isotropic materials without reflecting any anisotropic characteristics. In the elastic deformation phase,

according to (4), the modified PUFF equation of state which considers both nonlinear volume change and anisotropic property is obtained [4 - 6]:
compression region:

$$p = -A_1'\theta + \left(A_2 - A_1\Gamma_0/2\right)\theta^2 - \left(A_3 - A_2\Gamma_0/2\right)\theta^3 + \left(\rho_0\Gamma_0 - \rho_0\Gamma_0\theta\right)e - \left(c_{11}+c_{13}-c_{22}-c_{23}\right)\varepsilon_{11}^d/3 \quad (10)$$

expansion region:

$$p = -B_1'\theta + B_2\theta^2 - B_3\theta^3 + \left[\rho_0\Gamma_0 - 3\rho_0\Gamma_0\theta/2 + \rho_0\left(\gamma-1\right)\theta/2\right]e - \left(c_{11}+c_{13}-c_{22}-c_{23}\right)\varepsilon_{11}^d/3 \quad (11)$$

where $A_1' = B_1' = \left(c_{11}+3c_{12}+c_{13}+2c_{22}+2c_{23}\right)/9$. A_1' (B_1') reflects the anisotropic property and is called as effective bulk modulus.

Thus, for elastic response, the pressure can be gained from (10) and (11), and the deviatoric stresses are calculated by (5), then the total stresses gotten from $\sigma_{ij} = -p\delta_{ij} + s_{ij}$ can account for both nonlinear behaviour of volume change and anisotropic property.

III. Plane-strain Constitutive Model for Plastic Response

A. Plastic Constitutive Model

In the plastic deformation phase, the Hooke law is satisfied between stress increment and strain increment, so the constitutive relation can be depicted by increment form:

$$\begin{pmatrix} d\sigma_{11}\\ d\sigma_{22}\\ d\sigma_{33}\\ d\sigma_{12}\end{pmatrix} = \begin{pmatrix} c_{11} & c_{12} & c_{13} & 0\\ c_{12} & c_{22} & c_{23} & 0\\ c_{13} & c_{23} & c_{33} & 0\\ 0 & 0 & 0 & c_{44}\end{pmatrix}\begin{pmatrix} d\varepsilon_{11}^e\\ d\varepsilon_{22}^e\\ d\varepsilon_{33}^e\\ d\varepsilon_{12}^e\end{pmatrix} = \begin{pmatrix} c_{11} & c_{12} & c_{13} & 0\\ c_{12} & c_{22} & c_{23} & 0\\ c_{13} & c_{23} & c_{33} & 0\\ 0 & 0 & 0 & c_{44}\end{pmatrix}\begin{pmatrix} d\varepsilon_{11}-d\varepsilon_{11}^p\\ d\varepsilon_{22}-d\varepsilon_{22}^p\\ -d\varepsilon_{33}^p\\ d\varepsilon_{12}-d\varepsilon_{12}^p\end{pmatrix} \quad (12)$$

where $d\varepsilon_{ij}^e$ represents elastic strain increment, and $d\varepsilon_{ij}^p$ is plastic strain increment calculated by yield criterion which will be discussed later.

Also the stress increment is decomposed to pressure increment and deviatoric stress increment, then the pressure increment in plastic region can be written as:

$$\begin{aligned} dp &= -\left(d\sigma_{11}+d\sigma_{22}+d\sigma_{33}\right)\\ &= -\left(c_{11}+3c_{12}+c_{13}+2c_{22}+2c_{23}\right)d\theta/9\\ &\quad -\left(c_{11}+c_{13}-c_{22}-c_{23}\right)d\varepsilon_{11}^d/3\\ &\quad +\left(c_{11}+c_{12}+c_{13}\right)d\varepsilon_{11}^p/3+\left(c_{12}+c_{22}+c_{23}\right)d\varepsilon_{22}^p/3\\ &\quad +\left(c_{13}+c_{23}+c_{33}\right)d\varepsilon_{33}^p/3 \end{aligned} \quad (13)$$

From (13), it is clear to find that, for the anisotropic material, the pressure increment depends on not only volumetric strain increment, but also the deviatoric strain and plastic strain increment. In the limit of isotropic material, (13) reduces to $dp = -\kappa d\theta = -\dfrac{E}{3\left(1-2\upsilon\right)}d\theta$ ·

The deviatoric stress increment components are:

$$\begin{cases} ds_{11} = \left(2c_{11}+3c_{12}-c_{13}-2c_{22}-2c_{23}\right)d\theta/9\\ \qquad +\left(2c_{11}-3c_{12}-c_{13}+c_{22}+c_{23}\right)d\varepsilon_{11}^d/3\\ \qquad -\left(2c_{11}-c_{12}-c_{13}\right)d\varepsilon_{11}^p/3\\ \qquad -\left(2c_{12}-2c_{22}-2c_{23}\right)d\varepsilon_{22}^p/3\\ \qquad -\left(2c_{13}-c_{23}-c_{33}\right)d\varepsilon_{33}^p/3\\ ds_{22} = \left(-c_{11}-c_{13}+4c_{22}-2c_{23}\right)d\theta/9\\ \qquad +\left(-c_{11}+3c_{12}-c_{13}-2c_{22}+c_{23}\right)d\varepsilon_{11}^d/3\\ \qquad -\left(2c_{12}-c_{11}-c_{13}\right)d\varepsilon_{11}^p/3\\ \qquad -\left(2c_{22}-c_{12}-c_{23}\right)d\varepsilon_{22}^p/3\\ \qquad -\left(2c_{23}-c_{13}-c_{33}\right)d\varepsilon_{33}^p/3\\ ds_{33} = \left(-c_{11}-3c_{12}+2c_{13}-2c_{22}+4c_{23}\right)d\theta/9\\ \qquad +\left(-c_{11}+2c_{13}+c_{22}-2c_{23}\right)d\varepsilon_{11}^d/3\\ \qquad -\left(2c_{13}-c_{11}-c_{12}\right)d\varepsilon_{11}^p/3\\ \qquad -\left(2c_{23}-c_{12}-c_{22}\right)d\varepsilon_{22}^p/3\\ \qquad -\left(2c_{33}-c_{13}-c_{23}\right)d\varepsilon_{33}^p/3\\ ds_{12} = c_{44}\left(d\varepsilon_{12}-d\varepsilon_{12}^p\right) \end{cases} \quad (14)$$

Like Eq. (4), to consider both nonlinear behaviour of volume change and anisotropic property, the modified PUFF equation of state is introduced, and Eq. (13) is rewritten as:
compression region:

$$\begin{aligned} dp &= -A_1'd\theta + 2\left(A_2 - A_1\Gamma_0/2\right)\theta d\theta\\ &\quad -3\left(A_3 - A_2\Gamma_0/2\right)\theta^2 d\theta + \left(\rho_0\Gamma_0 - \rho_0\Gamma_0\theta\right)de\\ &\quad -\rho_0\Gamma_0 e d\theta - \left(c_{11}+c_{13}-c_{22}-c_{23}\right)d\varepsilon_{11}^d/3\\ &\quad +\left(c_{11}+c_{12}+c_{13}\right)d\varepsilon_{11}^p/3+\left(c_{12}+c_{22}+c_{23}\right)d\varepsilon_{22}^p/3\\ &\quad +\left(c_{13}+c_{23}+c_{33}\right)d\varepsilon_{33}^p/3 \end{aligned} \quad (15)$$

expansion region:

$$\begin{aligned} dp = & -B_1' d\theta + 2B_2 \theta d\theta - 3B_3 \theta^2 d\theta \\ & + \left[\rho_0 \Gamma_0 - 3\rho_0 \Gamma_0 \theta/2 + \rho_0 (\gamma - 1)\theta/2\right] de \\ & - \left[3\rho_0 \Gamma_0 / 2 - \rho_0 (\gamma - 1)/2\right] e d\theta \\ & - (c_{11} + c_{13} - c_{22} - c_{23}) d\varepsilon_{11}^d / 3 + (c_{11} + c_{12} + c_{13}) d\varepsilon_{11}^p / 3 \\ & + (c_{12} + c_{22} + c_{23}) d\varepsilon_{22}^p / 3 + (c_{13} + c_{23} + c_{33}) d\varepsilon_{33}^p / 3 \end{aligned} \tag{16}$$

After the deviatoric stress increment components and pressure increment are calculated from (14) – (16), the stress increment components can be obtained by $d\sigma_{ij} = -dp\delta_{ij} + ds_{ij}$. But the plastic strain increment must be gotten first, then the anisotropic yield criterion is discussed.

B. Rate-related Tsai-Hill Yield Criterion

For anisotropic materials, the Tsai-Hill yield criterion is used to judge whether the material has enter the plastic deformation state, and under condition of plane strain, the basic form is:

$$\begin{aligned} F = & \frac{{\sigma_{11}}^2}{Y_{11}^2} + \frac{{\sigma_{22}}^2}{Y_{22}^2} + \frac{{\sigma_{33}}^2}{Y_{33}^2} + \frac{{\sigma_{12}}^2}{Y_{12}^2} \\ & + \bar{Y}_{33}\sigma_{11}\sigma_{22} + \bar{Y}_{22}\sigma_{11}\sigma_{33} + \bar{Y}_{11}\sigma_{22}\sigma_{33} - 1 = 0 \end{aligned} \tag{17}$$

where $\bar{Y}_{11} = 1/Y_{11}^2 - 1/Y_{22}^2 - 1/Y_{33}^2$, $\bar{Y}_{22} = 1/Y_{22}^2 - 1/Y_{11}^2 - 1/Y_{33}^2$, $\bar{Y}_{11} = 1/Y_{33}^2 - 1/Y_{22}^2 - 1/Y_{11}^2$, Y_{11}, Y_{22}, Y_{33} are the yield strengths in three principal directions and Y_{12} is shear yield strength in 1-2 plane without considering strain rate effect, but they are related with strain hardening effect and equivalent plastic strain, i.e. $Y_{ij} = Y_{ij0}\left[1 + a_{ij}\left(\bar{\varepsilon}^p\right)^{n_{ij}}\right]$. Y_{ij0} are the initial yield strengths from quasi static experiments, a_{ij}, n_{ij} are the parameters reflecting the strain hardening property, and $\bar{\varepsilon}_p$ is the equivalent plastic strain defined as $\bar{\varepsilon}_p = \sqrt{2\varepsilon_{ij}^p \varepsilon_{ij}^p / 3}$.

Considering the strain rate sensitivity [7, 8], use $Y_{ij}\left(1 + \beta_{ij} \ln \dot{\varepsilon} / \dot{\varepsilon}_0\right)$ to represent the yield strengths at different strain rate, where β_{ij} is the parameter reflecting strain rate sensitivity from dynamic experiment, $\dot{\varepsilon}_0$ is the reference strain rate, and consider strain rate $\dot{\varepsilon}$ as effective plastic strain rate $\dot{\bar{\varepsilon}}_p = \sqrt{2\dot{\varepsilon}_{ij}^p \dot{\varepsilon}_{ij}^p / 3}$. For convenience of numerical simulation, we set β as the average value of β_{ij}, and strain rate factor is $R\left(\dot{\varepsilon}\right) = 1 + \beta \ln \dot{\varepsilon} / \dot{\varepsilon}_0$. Then the rate-rated Tsai-Hill yield criterion is:

$$\left(F + 1\right)/R^2 - 1 = 0 \tag{18}$$

Equation (18) can be rewritten as the rate separated yield criterion form:

$$f \equiv \dot{\varepsilon}_0 \exp\left[\frac{1}{\beta}\left(\sqrt{F+1} - 1\right)\right] - \dot{\varepsilon} = 0 \tag{19}$$

According to normality principle, the plastic strain increment is:

$$\begin{aligned} d\varepsilon_{ij}^p &= d\lambda \frac{\partial f}{\partial \sigma_{ij}} \\ &= d\lambda \dot{\varepsilon}_0 \exp\left[\left(\sqrt{F+1} - 1\right)/\beta\right]\left(1/2\beta\sqrt{F+1}\right) D_{ij} \end{aligned} \tag{20}$$

where $d\lambda = 2\beta\sqrt{F+1} / \sqrt{2D_{ij}D_{ij}/3}$ is plastic flow factor, and $D_{ij} = \partial F / \partial \sigma_{ij}$.

According to $d\bar{\varepsilon}_p = \sqrt{2d\varepsilon_{ij}^p d\varepsilon_{ij}^p / 3}$ and (20), we get $d\lambda = d\bar{\varepsilon}_p / \sqrt{\frac{2}{3}\frac{\partial f}{\partial \sigma_{ij}}\frac{\partial f}{\partial \sigma_{ij}}}$. Based on the consistent principle, when the material is in plastic deformation phase, stress states are always on the yield surface, i.e. f = 0, so $\dot{\bar{\varepsilon}}_p = \dot{\varepsilon}_0 \exp\left[\left(\sqrt{F+1} - 1\right)/\beta\right]$. Thus we get:

$$d\lambda = \frac{d\bar{\varepsilon}_p}{\sqrt{\frac{2}{3}\frac{\partial f}{\partial \sigma_{ij}}\frac{\partial f}{\partial \sigma_{ij}}}} = \frac{2\beta\sqrt{F+1}dt}{\sqrt{\frac{2}{3}D_{ij}D_{ij}}} \tag{21}$$

From (20) and (21), the plastic strain increments are obtained, then the pressure and deviatoric stress increments are easily gotten by using (14) – (16).

IV. Numerical Simulation and Discussions

A. Problem Simplification and Material Model

Assume that with enough distance from the nuclear explosion center, the approximately parallel X-ray radiates the cylinder shell surface along the vertical direction of axial line, thus a series of cirque profiles are formed (see Fig. 1). If the axial dimension is much larger than the radial direction, this problem can be simplified as plane-strain problem, and the thermal shock wave propagation property can be discussed within an arbitrary cirque (see Fig. 2).

TF composite material has three principal axes (use 1, 2, 3 denotation) respectively called as thickness, warp, and fill directions, and the system axes are denoted by (x, y, z). We make numerical simulations based on three model cases. At the beginning of radiation, For the first model called TF1, the material thickness direction is along the radial direction of cylinder shell, the warp is along circumferential direction, and the fill is along axial (z axis) direction. For the second model called TF2, the material warp is along the radial direction of cylinder shell, the fill is along circumferential direction, and the thickness is along axial (z axis) direction. For the third model

called TF3, the material fill is along the radial direction of cylinder shell, the thickness is along circumferential direction, and the warp is along axial (z axis) direction. The X-ray blackbody spectra are set as kT=1 keV and 3 keV, initial energy flux density is 200 J/cm^2, and the rectangular pulse width is 0.1 ms. The outer radius of cirque is 1cm, the inner radius is 0.8 cm, and the main material parameters are shown in Table I - III [9].

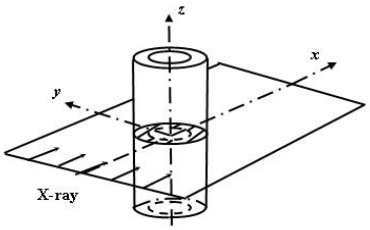

Fig. 1 Real model for cylinder shell under X-ray radiation

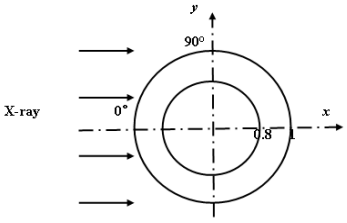

Fig. 2 Simplified model for numerical simulation

TABLE I
EOS PARAMETERS OF TF MATERIAL

Paramaters	Values	Paramaters	Values
ρ_0 (g/cm^3)	1.38	Γ_0	2.32
c_0 (km/s)	2.35	γ	1.4
s	1.66	e_s (kJ/g)	5.15

TABLE II
ELASTIC PARAMETERS OF TF MATERIAL

Paramaters	Values	Paramaters	Values
E_1 (GPa)	4.87	υ_{12}	0.28
E_2 (GPa)	6.96	υ_{23}	0.30
E_3 (GPa)	5.45	υ_{31}	0.313
G_{12} (GPa)	2.6	υ_{21}	0.40
G_{23} (GPa)	3.5	υ_{32}	0.235
G_{31} (GPa)	2.8	υ_{13}	0.28

TABLE III
PLASTIC PARAMETERS OF TF MATERIAL

Paramaters	Values	Paramaters	Values
Y_{110} (GPa)	0.17	a_{11}, n_{11}	8.5, 0.87
Y_{220} (GPa)	0.12	a_{22}, n_{22}	15.0, 0.85
Y_{330} (GPa)	0.063	a_{33}, n_{33}	11.0, 0.70
Y_{120} (GPa)	0.10	a_{12}, n_{12}	11.8,0.86
Y_{230} (GPa)	0.07	a_{23}, n_{23}	13.0, 0.78
Y_{310} (GPa)	0.08	a_{31}, n_{31}	10.0, 0.79
β	0.0218	$\dot{\varepsilon}_0$ (s^{-1})	0.001

B. Numerical Simulation Results and Discussions

Using the orthotropic elasto-plastic dynamic constitutive model, a 2-D finite element program is made to simulate the thermal shock wave propagation in TF material. The Profiles of σ_{xx} versus radius along the direction of 0° under radiation of 1 keV and 3 keV X-ray are given in Fig. 3- 6 (positive values represent compression). The contours of σ_{xx} are shown in Fig.7-10, and for the symmetry, only half of the cirque is displayed.

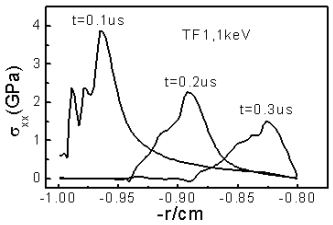

Fig. 3 Profiles of σ_{xx} in TF1 along the direction of 0° under radiation of 1 keV X-ray

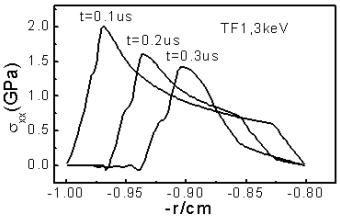

Fig. 4 Profiles of σ_{xx} in TF1 along the direction of 0° under radiation of 3 keV X-ray

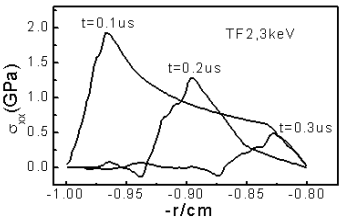

Fig. 5 Profiles of σ_{xx} in TF2 along the direction of 0° under radiation of 3 keV X-ray

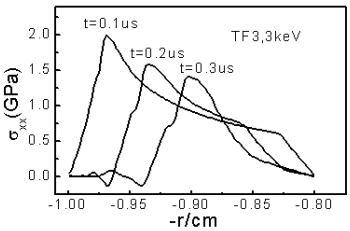

Fig. 6 Profiles of σ_{xx} in TF3 along the direction of 0° under radiation of 3 keV X-ray

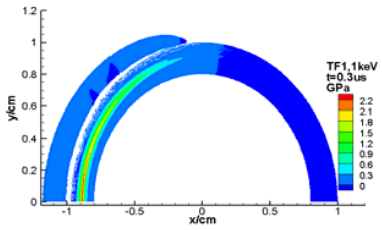

Fig. 7 Contour of σ_{xx} in TF1 under radiation of 1 keV X-ray

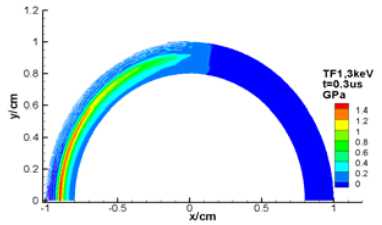

Fig. 8 Contour of σ_{xx} in TF1 under radiation of 3 keV X-ray

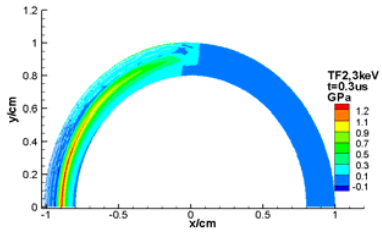

Fig. 9 Contour of σ_{xx} in TF2 under radiation of 3 keV X-ray

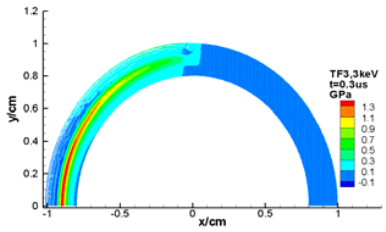

Fig. 10 Contour of σ_{xx} in TF2 under radiation of 3keV X-ray

From Fig. 3 - 4, we see that under the radiation of soft X-ray (1 keV), most energy deposites in the surface, the peak stress value is lager, the wave shape mainly appears as compression wave, and the triangle wave width is smaller; while under the radiation of hard X-ray (3 keV), the penetration capacity is better, so the energy deposition depth is deeper, the peak stress value is much lower, and a rarefaction wave is followed by the compression wave. From Figure 4 - Figure 6, we find that while the X-ray radiates material along different principal axes, there are obvious differences in stress wave propagation speed, peak stress values, attenuation speed, and so on. The propagation speed and attenuation of σ_{xx} in TF2 is fastest for the largest elastic modulus in warp direction.In Fig. 7, it is very intuitionistic to see that under radiation of soft X-ray, based on rapid X-ray energy deposition on the surface which has exceeded the sublimation energy of TF, the material surface is sublimated to gas immediately. But under radiation of hard X-ray, no sublimation phenomenon happens. In addition, from Fig. 8 - 10, the spallation in TF1 is much more serious, with a reason that the radius direction of TF1 is set as composite thickness principal axis whose mechanics property is mainly dominated by resin matrix with lower fracture strength, while the warp and fill axes are dominated by fibre whose fracture strengths are much lager.

V. Conclusion

A plane-strain orthotropic dynamic constitutive model which considers elasto-plastic deformation, strain rate sensitivity, strain hardening effect, and nonlinear property of volume change in both compression and expansion states is proposed in this paper. Taking the carbon fiber-reinforced phenolic composite composite for example, a 2-D finite element program is made to simulate the thermal shock wave propagation in cylinder shell under radiation of 1 keV and 3 keV X-ray, and the thermal shock wave propagation properties are discussed and obtained ultimately.The results show that the thermal shock wave exhibit different shapes under the radiation of soft and hard X-ray, especially for the sublimation phenomenon, and while the composite material is radiated along different principal axes, great differences exist in some aspects, such as wave propagation speed, attenuation of thermal shock wave peak value, spallation and so on.

References

[1] W. Tang, G. Zhao, and R. Zhang, "Thermal Shock Wave Induced by Impulsive X-ray (Periodical style), " *Chinese Journal of High Pressure Physics*, vol. 9(2), pp. 107-110, 1995.

[2] R. Zhang, W. Tang, and G. Zhao, "Several Influential Factors on Numerical Simulated Results for the X-rayThermal Shock Wave (Periodical style), " *Chinese Journal of High Pressure Physics*, vol. 12(3), pp. 161-167, 1998.

[3] N. Zhou, and D. Qiao, *Material Ddynamics under Pulse Beam Radiati*, (Book style). Beijing: National Defence Industry Press, 2002, pp. 207-210.

[4] P. E. O'Donoghue, C. E. Anderson, Jr., G. J. Friesenhahn, and C. H. Parr, "A Constitutive Formulation for Anisotropic Materials Suitable for Wave Propagation Computer Programs (Periodical style), *Journal of Composite Materials*, vol.26(13), pp. 1860-1884, 1992.

[5] C. E. Anderson, Jr., P. A. Cox, G. R. Johnson, and P. J. Maudlin, "A Constitutive Formulation for Anisotropic Materials Suitable for Wave Propagation Computer programs II (Periodical style)," *Computational Mechanics*, vol. 15, pp. 201-223, 1994.

[6] A. A. Lukyanov, "An Equation of State for Anisotropic Solids under Shock Loading (Periodical style)," *European Physical Journal*, vol.64, pp. 159-164, 2008.

[7] Y. Li, F. Tan, and L. Yao, "Thermo-viscoplastic Constitutive Relation of Damaged Materials with Application (Periodical style)," *Explosion and Shock Waves*, vol.24 (4), pp. 289 – 298, 2004.

[8] B. Jiang, and R. Zhang, "Strain Rate-dependent Tsai-Hill Strength Criteria for a Carbon Fiber Woven Reinforced Composite (Periodical style), "*Explosion and Shock Waves*, vol.26 (4), pp. 333-338, 2006.

[9] B. Jiang, "Research on dynamic constitutive model for an orthotropic woven fiber-reinforced composite and thermal shock wave," *Doctorate Degree Thesis*, National University of Defense Technology, Changsha, China, 2006.